http://dx.doi.org/10.5012/bkcs.2014.35.12.3514

DFT Calculated Structures and IR Spectra of the Conformers of *para*-Bromocalix[4]aryl Derivatives

Sangdoo Ahn,* Dong-Kuk Lee,† and Jong-In Choe*

Department of Chemistry, Chung-Ang University, Seoul 156-756, Korea
**E-mail: sangdoo@cau.ac.kr (S. Ahn); choeji@cau.ac.kr (J.-I. Choe)*
†Department of Fine Chemistry & Convergence Institute of Biomedical and Biomaterials, Seoul National University of Science and Technology, Seoul 139-743, Korea
Received March 11, 2014, Accepted August 17, 2014

Molecular structures of the various conformers of *para*-bromocalix[4]aryl derivatives **1–4** were optimized using the *DFT* B3LYP calculation method. The total electronic and Gibbs free energies and normal vibrational frequencies of the different structures (CONE, partial cone (PACO), 1,2-Alternate(1,2-A) and 1,3-Alternate(1,3-A)) were calculated from the four kinds of *para*-bromocalix[4]aryl derivatives. The B3LYP/6-31G(d,p) calculations suggested the following: **1**(PACO) is the most stable among four conformers of **1**; **2**(CONE) is the most stable among five conformers of **2**; **3**(PACO) is the most stable among four conformers of **3**; **4**(1,3-A) is the most stable among four conformers of **4**. All the most stable structures optimized by the B3LYP calculation method were in accordance with the experimental crystal structures of **1–4**. The calculated IR spectra of the various conformers (CONE, PACO, 1,2-A and 1,3-A) of **1–4** were compared.

Key Words : *DFT* B3LYP, Conformer, IR spectrum, Bromocalix[4]aryl derivatives

Introduction

Cavitand-type molecules contain a hydrophobic pocket, and whilst they can assemble into large nanometer-scale self-assembled architectures by non-covalent interactions, their ability to assemble into nanorafts is yet to be realized.[1] Calixarenes are a class of cavitands, often described as container molecules, cups, bowls, or molecular baskets; the cavities of calixarenes can function as receptors for the complexation of guest molecules.[2-5] However, many reported calixarene inclusion structures are actually lattice inclusion compounds where the guests occupy the spaces between the host molecules.[6,7] There are two reasons for this. First, the bowls of many common calixarenes are relatively small and hence cannot accept some guest molecules. Secondly, favorable host–guest interactions are required within the bowl for the complexation to be competitive with other crystal packing modes. One of the most active areas of calixarene research involves functionalization of the upper rim of the calix. Tetrabromo-tetramethoxycalix[4]arene methyl ether **1** serves as a precursor in the synthesis of thiocalixarenes *via* the reagent CUSEt.[8] Tetrabromo-dimethoxy-dihydroxycalix [4] arene **2** functions as a host molecule that simultaneously utilizes both the bowl receptor and lattice packing modes for molecular inclusion.[9,10] The four known conformations of calix[4]arenes–cone; partial-cone (PACO); 1,2-alternate (1,2-A); and 1,3-alternate (1,3-A)–have been extensively studied.[11-24]

In this study, we have optimized the various conformers (CONE, PACO, 1,2-A and 1,3-A) of four kinds of *para*-bromocalix[4]aryl derivatives **1–4** using B3LYP calculation methods. The primary objective of this research is to determine the structures and relative stabilities of different conformers of **1–4** using the B3LYP/6-31G(d,p) calculation method. The secondary objective is to compare the calculated IR spectra of four conformers of **1–4** obtained from the *DFT* B3LYP method. These findings might be useful for the design of receptors based on bromocalix[4]aryl derivatives for the construction of superstructures derived from hydrogen bonds.

Computational Methods

Four major conformations (CONE, PACO, 1,2-A and 1,3-A) of **1–4** were constructed using the molecular mechanics (MM), molecular dynamics (MD), and semi-empirical calculations of HyperChem.[25] Optimized structures were found by conformational searches using a previously described, simulated annealing method.[26] The conformers of **1–4** obtained from the MM/MD and AM1 calculations were fully re-optimized using the B3LYP/6-31G (d,p) calculation method to determine both the relative energies and structures of the distinct conformers.

Additional B3LYP/6-311+G(d,p) optimizations were performed using Gaussian 09[27] to obtain more accurate total electronic energies and structures for the conformers of **1–4**.

The B3LYP/6-31G(d,p) method was also used to calculate the normal mode frequencies of the final structures. The vibrational spectra showed no negative frequencies, confirming that the optimized structures exist in energy minima. For direct comparison with the experimental data, the calculated frequencies were scaled by the recommended scale factor (0.970).[28] Furthermore, broadened IR spectra are presented assuming a Lorentzian line width of 10 cm^{-1}.

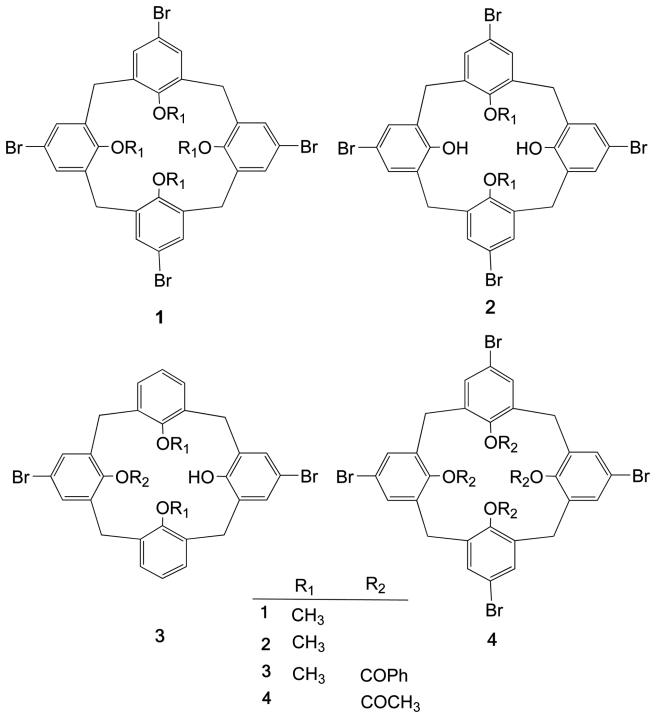

Scheme 1. Chemical structures of 5,11,17,23-tetrabromo-25,26,27,28-tetramethoxycalix[4]arene **1**, 5,11,17,23-tetrabromo-25,27-dimethoxy-26,28-dihydroxycalix[4] arene **2**, 5,17-dibromo-25-benzoyl-26,28-dimethoxy-27-hydroxycalix[4]arene **3**, and 5,11,17,23-tetrabromo-25,26,27,28-tetraacetoxycalix[4]arene **4**.

Results and Discussion

The structures of the various conformers of the four kinds of *para*-bromocalix[4]aryl derivatives **1–4** were optimized using the B3LYP/6-31G(d,p) calculation method to determine both the relative energies and structures of various distinct conformers.

Table 1 shows the optimized Gibbs free energies minimized by the B3LYP method with the 6-31G(d,p) basis set for the distinct conformational isomers.

The electronic energies of these structures were also optimized with larger 6-311+G(d,p) basis sets to obtain more accurate total electronic energies and structures for the conformers of **1–4**. Table 2 reports the additional B3LYP calculated total electronic energies of the various conformers of **1–4**.

Figure 1 shows the B3LYP/6-311+G(d,p) calculated structures of the most stable conformations (**1**(PACO), **2**(CONE), **3**(PACO) and **4**(1,3-A)) of **1–4**. Visualization of the optimized structures in Figure 1 was performed with PosMol[29] The frontier orbitals (HOMO and LUMO) for the most stable conformations were drawn by using GaussView.[30] "Supplementary Material" shows all the calculated structures and frontier orbitals (Figure S1) and IR spectra (Figures S2-S5) of the various conformers (CONE, PACO, 1,2-A and 1,3-A) of **1–4**.

The calculated Gibbs free energies in Table 1 suggest that **1**(PACO) is the most stable among the four conformations of 5,11,17,23-tetrabromo-25,26,27,28-tetramethoxycalix[4]arene **1**, which is in accord with the crystal structure of **1**.[8] The primary reason for the relative stabilities between the conformers of **1** is the steric hindrance of the methoxy group. The order of stability follows with the ΔG values (kcal/mol) in parentheses: **1**(PACO: most stable) < **1**(CONE: 1.53) < **1**(1,3-A: 2.45) < **1**(1,2-A: 4.08).

2(CONE) is the most stable among the five conformations

Table 1. *DFT* B3LYP/6-31G(d,p) Calculated Gibb Free Energies[a] of the Conformers for **1–4**

Conformer[b]	**1**		**2**		**3**		**4**	
	G	ΔG^c	G	ΔG^c	G	ΔG^c	G	ΔG^c
CONE	-11823.53049	1.53	-11745.00153	0.00	-6947.07686	1.91	-12277.40239	17.06
PACO	-11823.53293	0.00	-11744.99322	5.22	-6947.07991	0.00	-12277.42201	4.75
PACO2	not applicable		-11744.99529	3.92	not applicable		not applicable	
1,2-A	-11823.52642	4.08	-11744.99778	2.35	-6947.07931	0.38	-12277.42020	5.88
1,3-A	-11823.52902	2.45	-11744.98811	8.42	-6947.07420	3.58	-12277.42958	0.00

[a]The *DFT* B3LYP/6-31G(d,p) calculated Gibbs free energy at 298 K is expressed in Hartree (A.U). [b]Conformer: Compound **2** has two kinds of partial cone conformations: "PACO" implies partial cone with an inverted phenyl group, and "PACO2" denotes partial cone with an inverted anisole group. "1,2-A" means 1,2-alternate, etc. (See Figure 1). [c]ΔG (kcal/mol) is the relative energy with respect to the most stable conformation. Error limits in these calculations are about 0.01 kcal/mol.

Table 2. *DFT* B3LYP/6-311+G(d,p) Calculated Total Electronic Energies[a] of the Conformations for **1–4**

Conformer[b]	**1**		**2**		**3**		**4**	
Host	E	ΔE^c	E	ΔE^c	E	ΔE^c	E	ΔE^c
CONE	-11834.08525	1.17	-11755.49777	0.00	-6952.87782	3.77	-12287.64188	11.39
PACO	-11834.08711	0.00	-11755.48800	6.13	-6952.88383	0.00	-12287.65610	2.46
PACO2	not applicable		-11755.49087	4.33	not applicable		not applicable	
1,2-A	-11834.08017	4.36	-11755.49314	2.90	-6952.87964	2.63	-12287.65374	3.94
1,3-A	-11834.08273	2.75	-11755.48317	9.16	-6952.87590	4.98	-12287.66003	0.00

[a]The *DFT* B3LYP/6-311+G(d,p) calculated total electronic energy is expressed in Hartree (A.U). [b]Conformer: See the footnote of Table 1. [c]ΔE (kcal/mol) is the relative energy with respect to the most stable conformation. Error limits in these calculations are about 0.01 kcal/mol.

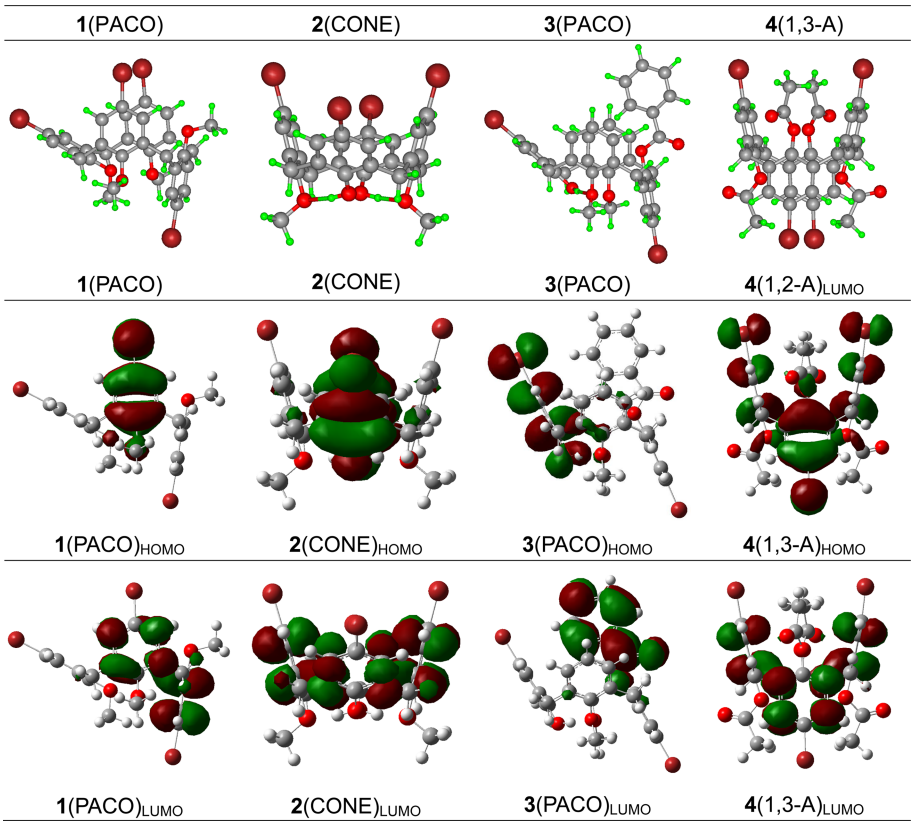

Figure 1. *DFT* B3LYP/6-311+G(d,p) calculated structures of the most stable conformations (**1**(PACO), **2**(CONE), **3**(PACO) and **4**(1,3-A)) of *para*-bromocalix[4]aryl derivatives (**1-4**). The visualization of the optimized structures was performed with PosMol.[29] (Atom: color; C: gray, H: green, O: red, Br: brown.) The frontier orbitals (HOMO and LUMO) for the various conformations are drawn by GaussView.[30] (Atom: color; C: gray, H: light gray, O: red, Br: brown.)

of 5,11,17,23-tetrabromo-25,27-dimethoxy-26,28-dihydroxycalix[4]arene **2**, which agrees with the experimental crystal structure of **2**.[9] The primary reason for the relative stabilities between the conformers of **2** is the degree of hydrogen bonding in the respective conformation. As evident from the optimized molecular structures in the second column of Figure S1, **2**(CONE) and **2**(1,2-A) have two H-bonds, while **2**(PACO) and **2**(PACO2) have one hydrogen bond. The least stable **2**(1,3-A) has no hydrogen bond. The order of stability follows with the ΔG values (kcal/mol) in parentheses: **2**(CONE: most stable) < **2**(1,2-A: 2.35) < **2**(PACO2: 3.92) < **2**(PACO: 5.21) < **2**(1,3-A: 8.42).

3(PACO) is the most stable of the four conformations of 5,17-dibromo-25-benzoyl-26,28-dimethoxy-27-hydroxycalix[4]arene **3**, which is in accord with the crystal structure of **3**.[10] Two reasons for the relative stabilities between the conformers of **3** are the steric hindrance of the benzoyl group with the phenyl rings and the number of hydrogen bonds in the respective conformation. As seen in the optimized molecular structures in the third column of the Figure S1, **3**(PACO) and **3**(1,2-A) have one hydrogen bond, while **3**(CONE) and **3**(1,3-A) have none. The order of stability follows the ΔG values (kcal/mol) in parentheses: **3**(PACO: most stable) ~ **3**(1,2-A: 0.38) < **3**(CONE: 1.91) < **3**(1,3-A: 3.58).

4(1,3-A) is the most stable among the four conformations of 5,11,17,23-tetrabromo-25,26,27,28-tetraacetoxycalix[4]arene **4**, which is in accord with the crystal structure of **4**.[11] The primary reason for the relative stabilities between the conformers of **4** is the steric hindrance of the acetoxy groups. **4**(CONE) is the least stable because it has four acetoxy groups oriented in the same direction. The order of stability follows with the ΔG values in parentheses: **4**(1,3-A: most stable) < **4**(PACO: 2.46) < **4**(1,2-A: 3.94) < **4**(CONE: 11.39 kcal/mol).

The B3LYP/6-31G(d,p) calculated IR spectra of the most stable conformers [**1**(PACO), **2**(CONE), **3**(PACO), **4**(1,3-A)] are compared in Table 3.

Calculated IR Spectrum of *para*-tetrabromo-tetramethyl-calix[4]arene 1(PACO): The IR spectra of the four conformers of **1**, whose structures are drawn in the first column of Figure S1, are shown in Figures S2(a)–S2(d). In the first column of Table 3, the prominent peaks of the most stable conformer (**1**(PACO)) are listed. See Figure 2. The weak peak at 532 cm^{-1} arises from the phenyl-ring breathing vibrations of the calix[4]aryl skeleton. The medium peak at 834 cm^{-1} is caused by C-Br stretching vibrations. The peak at 1013 cm^{-1} arises from the C-O bond stretching vibrations of the methoxy group. The peaks at 1152 and 1191 cm^{-1} arise from the vibrations of C-O bond stretching between the carbon atom in the phenyl ring and the oxygen atom. The peaks at 1424 and 1463 cm^{-1} arise from the concerted vib-

Table 3. Calculated Vibrational Frequencies[a] and Intensities[b] of the Most Stable Conformers of **1**–**4**, Respectively

1(PACO) Fig. 2		**2**(CONE) Fig. 3		**3**(PACO) Fig. 4		**4**(1,3-A) Fig. 5
Energy/cm^{-1}	Intensity	Energy/cm^{-1}	Vibrational modes	Energy/cm^{-1}	Intensity	Energy/cm^{-1}
		563	OH wagging /Ring breathing	554	weak	555
532	weak	641	Ring breathing	706	weak	757
834	medium	833	C-Br stretching	838, 846	medium	850
1013	medium	1008	C_{me}-O stretching	1003, 1019	strong	997
1152	medium	1148	C_{bz}-O stretching	1165	medium	1168
1191	strong	1209	C_{bz}-O stretching, C-C_{ar} stretching	1252	strong	1196
1424, 1463	strong	1467	C_{me}-O stretching + C_{bz}-O stretching	1462	strong	1447
1571	medium	1575	C-C stretching	1575	medium	1571
			C=O stretching	1748	strong	1783
2922	strong	2928	Symmetric C-H stretchings	2942	medium	2960
2984	medium, broad	2955	Antisymmetric C-H stretchings	2975	weak	3085
		3505	H-bonded O-H stretching	3437	very strong	
		3618 (PACO1)	Unrestricted O-H stretching	3632 (1,3-A)		

[a]The *DFT* calculated frequencies were scaled by the recommended scale factor (0.970).[31] [b]Calculated IR intensities from the *DFT* B3LYP/6-31G(d,p) method by the broadened IR spectra assuming a Lorentzian line width of 10 cm^{-1}.

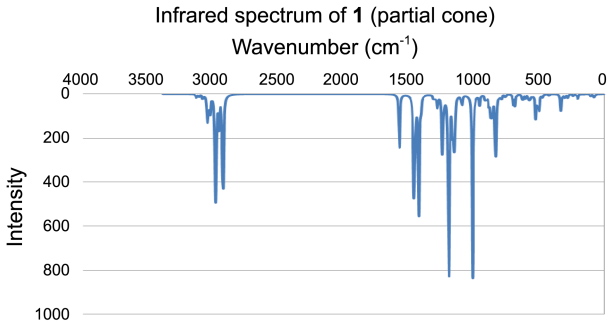

Figure 2. The *DFT* B3LYP/6-31G(d,p) calculated IR spectrum of the PACO conformer of *para*-tetrabromo-tetramethylcalix[4]arene **1**.

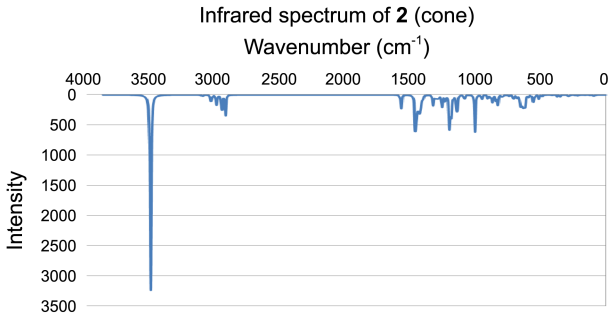

Figure 3. The *DFT* B3LYP/6-31G(d,p) calculated IR spectrum of the CONE conformer of *para*-tetrabromo-1,3-dimethylcalix[4] arene **2**.

rations of different C_{me}-O and C_{ph}-O bond stretchings. The peak at 1571 cm^{-1} arises from the vibrations of C-C bond stretching in the phenyl rings. The strong peaks at 2922 and 2984 cm^{-1} are composed of weak-intensity lines of the C-H symmetric and antisymmetric stretching vibrations in the methyl groups, respectively.

Calculated IR Spectrum of *para*-tetrabromo-dimethyl calix[4]arene 2: In the third column of Table 3, the prominent peaks of the most stable conformer (**2**(CONE)) are listed. See Figure 3. The main IR spectral features (frequencies and intensities plotted in Figures S3(a)–S3(e)) of the five conformers (drawn in the second column of Figure S1) differ slightly between each other in the lower-frequency range, except for the O-H wagging motion at 563 cm^{-1}. However, as observed in Table 4, the peaks at 3440–3548 cm^{-1}, corresponding to the restricted O-H bond stretching of the four different conformers, are red-shifted from the unrestricted O-H vibrational frequency (3618 cm^{-1}). In order to compare the hydrogen bond strengths of the different conformations, H-bond distances are reported in parentheses below the O-H vibrational frequencies in Table 4. The degree of discrepancy depends on the relative strength of hydrogen bond between the hydroxyl hydrogen atom and the methoxy oxygen. In Table 4, **2**(CONE) shows only an O-H bond stretching peak (doubly degenerate) at 3505 cm^{-1}, while **2**(PACO) shows two different O-H bond stretching peaks at

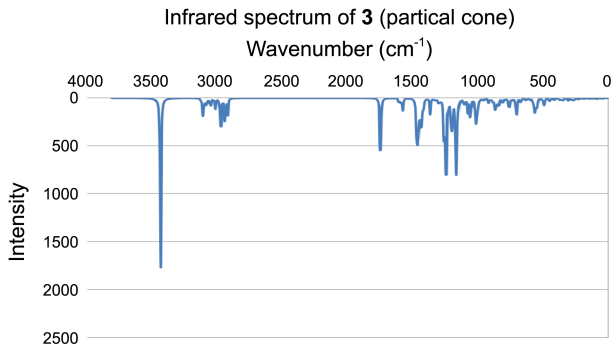

Figure 4. The *DFT* B3LYP/6-31G(d,p) calculated IR spectrum of the PACO conformer of 5,17-dibromo-25-benzoyl-26,28-dimethoxy-27-hydroxycalix[4]arene **3**.

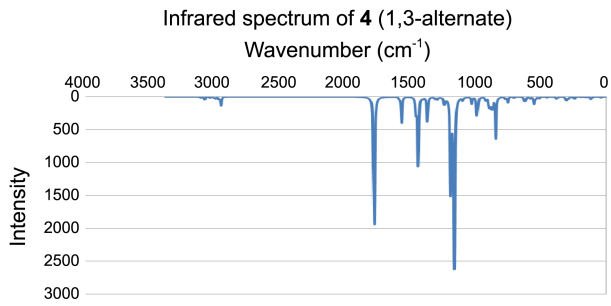

Figure 5. The *DFT* B3LYP/6-31G(d,p) calculated IR spectrum of the 1,3-A conformer of *para*-tetrabromocalix[4]arene methyl ester **4**.

3505 and 3618 cm^{-1}, due to the restricted and unrestricted vibrations of the H-bond. **2**(PACO2) shows an O-H bond stretching doublet at 3522 and 3548 cm^{-1}, corresponding to two different restricted vibrations resulting from the two slightly different H-bonds (two hydrogen bonds between two hydroxyl hydrogen atoms and a methoxy-oxygen). **2**(1,2-A) shows an O-H bond stretching peak at 3440 cm^{-1}, whose vibration frequency is much lower than that of the free O-H bond stretching (3618 cm^{-1}), because of the strongest H-bond (1.792 A) among the five different conformers of **2**.

Calculated IR Spectrum of 5,17-Dibromo-25-benzoyl-26,28-dimethoxy-27-hydroxycalix[4]arene 3: The IR spectra of the four conformers of **3**, whose structures are drawn in the third column of Figure 1, are shown in Figures S4(a)-S4(d). In the seventh column of Table 3, the prominent peaks of the most stable conformer (**3**(PACO)) are listed. See Figure 4. The weak peak at 711 cm^{-1} arises from the phenyl-ring breathing vibrations of the calix[4]aryl skeleton. The medium peaks at 842 and 850 cm^{-1} are caused by C-Br stretching vibrations. The strong peaks at 1008 and 1051 cm^{-1} arise from the C-O bond stretching vibrations of the methoxy group. The peak at 1165 cm^{-1} arises from the vibrations of C-O bond stretching between the carbon atom in the phenyl ring and the oxygen atom. The peak at 1462 cm^{-1} arises from the concerted vibration of different C_{me}-O and C_{ph}-O bond stretchings. The peak at 1575 cm^{-1} arises from the vibrations of C-C bond stretching in the phenyl rings. The strong peak at 1745 cm^{-1} arises from C=O bond stretching vibrations. The strong peaks 2937 and 2981 cm^{-1} are composed of weak-intensity lines of the C-H symmetric and antisymmetric stretching vibrations in the methyl groups, respectively. As observed in Table 5, the peaks at 3437–3461

Table 4. Calculated O-H Stretching Vibrational Frequencies[a] and O-H Distances of the Five Conformers of **2**

2(CONE) Fig. 3 & Fig. S3(a)		**2**(PACO1) Fig. S3(b)	**2**(PACO2) Fig. S3(c)	**2**(1,2-A) Fig. S3(d)	**2**(1,3-A) Fig. S3(e)
3505[b]	H-bonded O-H stretching	3505	3522, 3548	3440[b]	
1.824 Å, 1.824 Å	Calculated H-bonded O-H distance	1.814 Å	1.863 Å, 1.863 Å	1.792 Å, 1.792 Å	
1.839 Å, 1.772 Å	Experimental[9] O-H distance				
	Unrestricted O-H stretching	3618			3627[b]

[a]Unit of vibrational frequency is expressed in wavenumber (cm^{-1}). [b]Doubly degenerate.

Table 5. Calculated O-H Stretching Vibrational Frequencies[a] and O-H Distances of the Four Conformers of **3**

3(CONE) Fig. S4(a)		**3**(PACO) Fig. 4 & Fig. S4(b)	**3**(1,2-A) Fig. S4(c)	**3**(1,3-A) Fig. S4(d)
3461	H-bonded O-H stretching	3437	3447	
1.825 Å	Calculated H-bonded O-H distance	1.784 Å	1.830 Å	
	Unrestricted O-H stretching			3632

[a]Unit of vibrational frequency is expressed in wavenumber (cm^{-1}).

Table 6. *DFT* Calculated C=O Stretching Vibrational Frequencies[a] of the Four Conformers of **4**

4(CONE) Fig. S5(a)	**4**(PACO) Fig. S5(b)	**4**(1,2-A) Fig. S5(c)	**4**(1,3-A) Fig. 5 & Fig. S5(d)
1784 (doublet), 1800 (doublet)[b]	1786-1804 (broard)	1792 (close quartet)[c]	1784 (singlet)[d]

[a]Unit of vibrational frequency is expressed in wavenumber (cm^{-1}). [b]Two kinds of C=O stretching vibrational motions due to C_s symmetry. The cone is not square, but rectangle. [c]Four kinds of symmetric and antisymmetric double C=O stretching vibrational motions. [d]Four kinds of symmetric and antisymmetric C=O stretching vibrational motions in similar frequencies.

cm^{-1}, corresponding to the restricted H-bonded O-H bond stretching of the three different conformers, are red-shifted from the unrestricted O-H vibrational frequency (3632 cm^{-1}). In the Table, **3**(CONE) of Figure S4(a) shows one O-H bond stretching peak at 3461 cm^{-1}, **3**(PACO) of Figure S4(b) also shows an O-H peak at 3437 cm^{-1}, and **3**(1,2-A) of Figure S4(c) shows an O-H peak at 3447 cm^{-1}, due to the restricted O-H vibrational motion by the H-bond. These vibrational frequencies are much lower than that of the free O-H bond stretching (3632 cm^{-1}) of **3**(1,3-A) of Figure S4(d).

Calculated IR Spectrum of *para*-Tetrabromocalix[4] arenyl ester 4: The IR spectra of the four conformers of **4**, whose structures are drawn in the last column of Figure 1, are shown in Figures S5(a)-S(d). In the last column of Table 3, the prominent peaks of the most stable conformer (**4**(1,3-A)) are listed. See Figure 5. The weak peaks at 555 and 757 cm^{-1} arise from the phenyl-ring breathing vibrations of the calix[4]aryl skeleton. The medium peak at 850 cm^{-1} is caused by C-Br stretching vibrations. The medium peak at 997 cm^{-1} arises from the C-O bond stretching vibrations of the methyl ester group. The strong peak at 1168 arises from the vibrations of C_{ph}-O bond stretching between the carbon atom in the phenyl ring and the oxygen atom. The strong peak at 1196 cm^{-1} arises from the vibrations of C-O bond stretching in the ester group. The peak at 1447 cm^{-1} arises from C_{ph}-O bond stretching vibrations. The peak at 1571 cm^{-1} arises from the vibrations of C-C bond stretching in the phenyl rings. As observed in Table 6, the peaks at 1784 and 1800 cm^{-1} of **4**(CONE) of Figure S5(a) arise from two kinds of C=O bond stretching vibrational motions due to C_s symmetry, since the cone is not square, but rectangle. The broad peak between 1786 and 1804 cm^{-1} of **4**(PACO) of Figure S5(b) arises from two kinds of symmetric and antisymmetric C=O bond stretching vibrational motions. A big peak at 1792 cm^{-1} of **4**(1,2-A) of Figure S5(c) arises from the close quartet of four kinds of symmetric and antisymmetric double C=O bond stretching vibrational motions. A big peak at 1784 cm^{-1} of **4**(1,3-A) of Figure S5(d) arises from four kinds of symmetric and antisymmetric C=O bond stretching vibrational motions in very similar frequencies. The strong peaks 2960 and 3085 cm^{-1} of **4**(1,3-A) are composed of the weak-intensity lines of C-H symmetric and antisymmetric stretching vibrations in the methyl groups, respectively.

Conclusion

The total electronic and Gibbs free energies and normal vibrational frequencies of different structures of the four major conformations (CONE, PACO, 1,2-A and 1,3-A) of **1**–**4** were calculated using B3LYP methods. **1**(PACO) is the most stable among the four conformations of **1**; **2**(CONE) is the most stable among the five conformers of **2**; **3**(PACO) is the most stable of the four conformations of **3**; and **4**(1,3-A) is the most stable among the four conformers of **4**. All of the most stable structures optimized by the B3LYP calculation method are in accord with the crystal structures of **1-4**, respectively. The calculated IR spectra of the various conformers (CONE, PACO, 1,2-A and 1,3-A) of **1-4** were also compared.

Acknowledgments. Publication cost of this paper was supported by the Korean Chemical Society.

Supplementary Material. All the calculated structures (Figure S1) and IR spectra (Figures S2-S5) of the various conformers (CONE, PACO, 1,2-A and 1,3-A) of the four kinds of *para*-bromocalix[4]aryl derivatives (1–4).

References

1. Cram, D. J. *Science* **1983**, *219*, 1177.
2. Gutsche, C. D. *Calixarenes*; Royal Society of Chemistry: Cambridge, 2008.
3. Atwood, J. L., Davies, J. E. D., MacNicol, D. D., Eds.; *Inclusion Compounds*; Academic Press: London, 1984; vol. 1-3.
4. Atwood, J. L., Davies, J. E. D., MacNicol, D. D., Eds.; *Inclusion Compounds*; Oxford University Press: Oxford, 1991; vol. 4-5.
5. Atwood, J. L., Davies, J. E. D., MacNicol, D. D., Vögtle, F., Eds.; *Comprehensive Supramolecular Chemistry*; Pergamon: Oxford, 1996; vol. 1-11.
6. Perrin, M.; Dehler, O., *Topics in Inclusion Science*, In: Vicens, J., Böhmer, V., Eds.; Calixarenes: A Versatile Class of Macrocyclic Compounds, Kluwer, Dordrecht, 1991; pp 65-85.
7. Pochini, A.; Ungaro, R., *Calixarenes and Related Hosts*, In: Vögtle, F., Ed.; *Comprehensive Supramolecular Chemistry*; Pergamon: Oxford, 1996; vol. 2, pp 103-142.
8. Hamada, F.; Bott, S. G.; William, G.; Coleman, A. W.; Zhang, H.; Atwood, J. L. *J. Incl. Phenom. Mol. Reco.* **1990**, *9*, 195.
9. Maharaj, F.; Craig, D. C.; Scudder, M. L.; Bishop, R. N. K. *J. Incl. Phenom. Macrocyl. Chem.* **2007**, *59*, 17.
10. Yu, F.-J.; Hu, X.-J.; Yang, H.-J.; Wang, R.-J. *J. Kristallogr.-New Cryst. Struct.* **2005**, *220*, 460.
11. Clark, T. E.; Makha, M.; Sobolev, A. N.; Rohrs, H.; Atwood, J. L.; Raston, C. L. *Chem. Eur. J.* **2008**, *14*, 3931.
12. Iwamoto, K; Araki, K.; Shinkai, S. *J. Org. Chem.* **1991**, *56*, 4955.
13. Shinkai, S.; Iwamoto, K.; Araki, K.; Matsuda, T. *Chem. Commun.* **1990**, 1263.
14. Grootenhuis, P. D. J.; Kollman, P. A.; Groenen, L. C.; Reinhoudt, D. N.; van Hummel, G. J.; Ugazzoli, F.; Andreetti, G. D. *J. Am. Chem. Soc.* **1990**, *112*, 4165.

15. Groenen, L. C.; van Loon, J.-D.; Verboom, W.; Harkema, S.; Casnati, A.; Ungaro, R.; Pochini, A.; Ugozzoli, F.; Reinhoudt, D. N. *J. Am. Chem. Soc*. **1991,** *113*, 2385.
16. Hay, B. P.; Nicholas, J. B.; Feller, D. *J. Am. Chem. Soc*. **2000**, *122*, 10083.
17. Minn, H. H.; Chang, S. K.; No, K. T. *Theor. Chim. Acta* **1989**, *75*, 233.
18. Bernardino, R. J.; Costa Cabral, B. J.; Pereira, J. L. C. *Theochem*. **1998**, *455*, 23.
19. Scheerder, J.; Vreekamp, R. H.; Engbersen, J. F. J.; Verboom, W.; van Duynhoven, J. P. M.; Reinhoudt, D. N. *J. Org. Chem*. **1996**, *61*, 3476.
20. Fischer, S.; Grootenhuis, P. D. J.; Groenen, L. C.; van Hoorn, W. P.; van Veggel, F. C. J. M.; Reinhoudt, D. N.; Karplus, M. *J. Am. Chem. Soc*. **1995**, *117*, 1611.
21. Harada, T.; Shinkai, S. *J. Chem. Soc., Perkin Trans. 2* **1995**, 2231.
22. Thondorf, I.; Brenn, J.; Brandt, W.; Böhmer, V. *Tetrahedron Lett.* **1995**, *36*, 6665.
23. Iwamoto, K.; Ikeda, A.; Araki, K.; Harada, T.; Shinkai, S. *Tetrahedron* **1993**, *49*, 9937.
24. Harada, T.; Rudziński, J. M.; Osawa, E.; Shinkai, S. *Tetrahedron* **1993**, *49*, 5941.
25. *HyperChem Release 8*, Hypercube, Inc.: Waterloo, Ontario, Canada, 2009.
26. Choe, J.-I.; Kim, K.; Chang, S.-K. *Bull. Korean Chem. Soc*. **2000**, *21*, 465.
27. Frisch, M. J.; Trucks, G. W.; Schlegel, H. B.; Scuseria, G. E.; Robb, M. A.; Cheeseman, J. R.; Montgomery, J. A., Jr.; Vreven, T.; Kudin, K. N.; Burant, J. C.; Millam, J. M.; Iyengar, S. S.; Tomasi, J.; Barone, V.; Mennucci, B.; Cossi, M.; Scalmani, G.; Rega, N.; Petersson, G. A.; Nakatsuji, H.; Hada, M.; Ehara, M.; Toyota, K.; Fukuda, R.; Hasegawa, J.; Ishida, M.; Nakajima, T.; Honda, Y.; Kitao, O.; Nakai, H.; Klene, M.; Li, X.; Knox, J. E.; Hratchian, H. P.; Cross, J. B.; Bakken, V.; Adamo, C.; Jaramillo, J.; Gomperts, R.; Stratmann, R. E.; Yazyev, O.; Austin, A. J.; Cammi, R.; Pomelli, C.; Ochterski, J. W.; Ayala, P. Y.; Morokuma, K.; Voth, G. A.; Salvador, P.; Dannenberg, J. J.; Zakrzewski, V. G.; Dapprich, S.; Daniels, A. D.; Strain, M. C.; Farkas, O.; Malick, D. K.; Rabuck, A. D.; Raghavachari, K.; Foresman, J. B.; Ortiz, J. V.; Cui, Q.; Baboul, A. G.; Clifford, S.; Cioslowski, J.; Stefanov, B. B.; Liu, G.; Liashenko, A.; Piskorz, P.; Komaromi, I.; Martin, R. L.; Fox, D. J.; Keith, T.; Al-Laham, M. A.; Peng, C. Y.; Nanayakkara, A.; Challacombe, M.; Gill, P. M. W.; Johnson, B.; Chen, W.; Wong, M. W.; Gonzalez, C.; Pople, J. A. *Gaussian 09*, Revision C.01, Gaussian, Inc., Wallingford CT, 2009.
28. Foresman, J. B.; Frisch, A. *Exploring Chemistry with Electronic Structure Methods (Second Edition)*; Gaussian, Inc. Pittsburgh, PA, 1996; p 63.
29. Lee, S. J.; Chung, H. Y.; Kim, K. S. *Bull. Korean Chem. Soc.* **2004**, *25*, 1061.
30. GaussView, Version 5, Dennington, Roy; Keith, Todd; Millam, John. Semichem Inc., Shawnee Mission, KS, 2009.